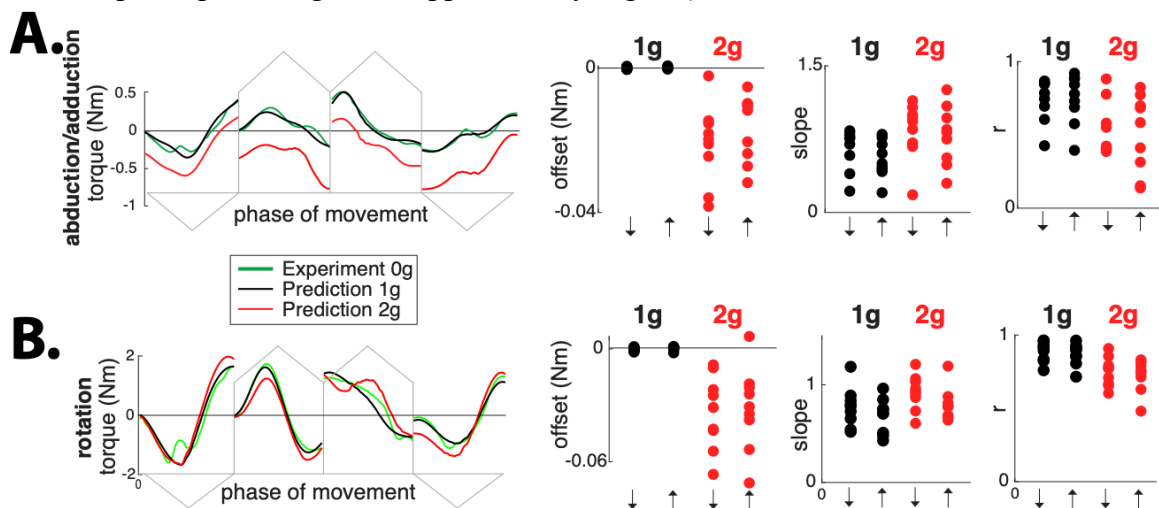


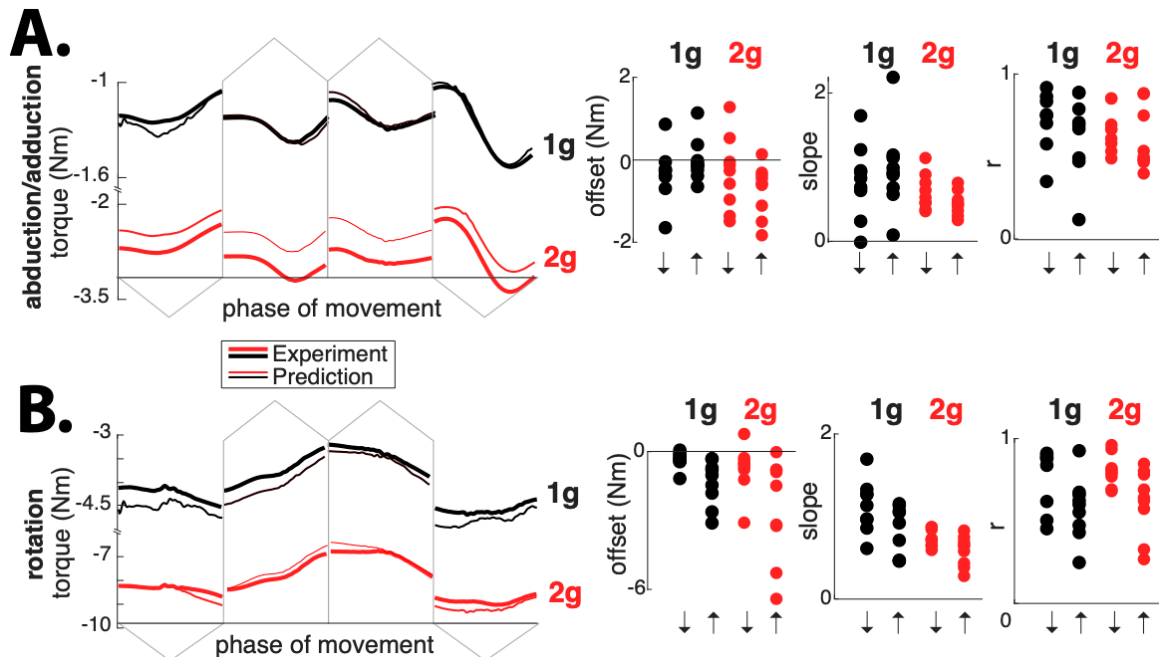
Supplementary Materials

Joint torque about the shoulder

Participants executed upward and downward pointing movements during microgravity (0g), normogravity (1g), and hypergravity (2g) phases of parabolic flight while arm motion capture and electromyographic (EMG) activity from shoulder muscles were recorded. Inverse-dynamics (ID) analysis of motion capture data showed that the gravity-independent dynamic component of joint torques remained highly similar across movement directions and gravitational conditions (Fig. 2A,B, Supplementary Fig. S1). Linear regressions between experimentally measured torques and model-predicted dynamic torques yielded Pearson correlation coefficients and slopes close to unity in most cases ($p < 0.01$ for all participants and degrees of freedom; Fig. 2B, Supplementary Fig. S1). In contrast, the gravity-related component of joint torques scaled systematically with gravitational acceleration (Fig. 2C; Supplementary Fig. S2), producing larger torque magnitudes under higher gravitational loads. Although the temporal profiles of gravity-related torques remained similar across conditions, regression slopes and correlation coefficients were more variable, particularly during upward movements ($p < 0.01$ for 7 out of 8 participants; Fig. 2C, Supplementary Fig. S2).



Supplementary Figure S1. A. Trajectories show examples of abduction/adduction shoulder torque profiles derived from ID during the 0g condition (thick green line) and the predicted dynamics from simulations using the data during the 1g and 2g conditions (thin black and red lines respectively) for one participant. Scatter plots show linear regression metrics (offset, slope, and Pearson correlation coefficient r) between experimental and predicted profiles for upward and downward movements indicated by arrows for the same DOF, symbols show data for participants. B. Same as A but for internal/external rotation of the shoulder.



Supplementary Figure S2. A. Trajectories show examples of abduction/adduction shoulder torque profiles derived from ID during the 1g and 2g conditions (thick black and red lines respectively) and the predicted gravity load from simulations using the data during the 2g and 1g condition (thin black and red lines respectively) for one participant. Scatter plots show linear regression metrics (offset, slope, and Pearson correlation coefficient r) between experimental and predicted profiles for upward and downward movements indicated by arrows for the same DOF, symbols show data for participants. B. Same as A but for internal/external rotation of the shoulder.

Estimates of stability

Variability of the dynamic torque component increased with gravitational load, as reflected by the highest standard deviations of ID-derived torques at 2g condition (Supplementary Table S1; paired t-test across all DOFs and subjects: $t = 2.29$, $p = 0.024$ for 2g relative to 1g and $t = 0.70$, $p = 0.485$ for 0g relative to 1g).

Supplementary Table S1: Standard deviation across time of dynamic torques derived from inverse dynamics.

| Shoulder DOF | Direction | 0g | 1g | 2g |
|----------------------------|-----------|-------------------|-------------------|-------------------|
| Extension/Flexion | down | 0.036 ± 0.009 | 0.034 ± 0.008 | 0.038 ± 0.008 |
| | up | 0.041 ± 0.011 | 0.039 ± 0.009 | 0.043 ± 0.012 |
| Abduction/Adduction | down | 0.004 ± 0.002 | 0.003 ± 0.001 | 0.008 ± 0.003 |
| | up | 0.005 ± 0.003 | 0.003 ± 0.002 | 0.009 ± 0.005 |
| External/Internal Rotation | down | 0.013 ± 0.007 | 0.011 ± 0.005 | 0.021 ± 0.007 |
| | up | 0.016 ± 0.008 | 0.013 ± 0.006 | 0.024 ± 0.008 |

DOF – degree of freedom; the range is standard deviation across participants; 0g, 1g, 2g denote phases of parabolic flight.

Similar trend was observed for the EMG-derived torques with the lowest standard deviations at 0g (Supplementary Table S2; paired t-test across all DOFs and subjects: $t = 2.24, p = 0.027$ for 1g relative to 0g and $t = 1.98, p = 0.050$ for 2g relative to 1g).

Supplementary Table S2: Standard deviation across time of dynamic torques derived from electromyography.

| Shoulder DOF | Direction | 0g | 1g | 2g |
|----------------------------|-----------|---------------|---------------|---------------|
| Extension/Flexion | down | 0.023 ± 0.015 | 0.031 ± 0.008 | 0.051 ± 0.015 |
| | up | 0.039 ± 0.013 | 0.059 ± 0.028 | 0.076 ± 0.027 |
| Abduction/Adduction | down | 0.010 ± 0.008 | 0.015 ± 0.011 | 0.019 ± 0.011 |
| | up | 0.012 ± 0.008 | 0.016 ± 0.010 | 0.021 ± 0.011 |
| External/Internal Rotation | down | 0.009 ± 0.005 | 0.013 ± 0.006 | 0.017 ± 0.007 |
| | up | 0.015 ± 0.009 | 0.021 ± 0.010 | 0.025 ± 0.013 |

DOF – degree of freedom; the range is standard deviation across participants; 0g, 1g, 2g denote phases of parabolic flight.

Torque prediction statistics

Mixed-effects analysis of gravity-related and dynamic torque components revealed distinct gravity scaling and systematic differences between inverse-dynamics (ID)- and EMG- derived estimates (Fig. 7). For the integrated gravity component, a significant main effect of derivation method was observed ($F(1,1491) = 5.36, p = 0.021$; Supplementary Table S3). The main effect of gravity condition was not significant ($F(1,1491) = 0.11, p = 0.74$), consistent with a largely constant offset between gravity components derived from EMG and those predicted from kinematics using inverse dynamics. However, a strong method × gravity interaction was present ($F(1,1491) = 147.89, p = 1.64 \times 10^{-32}$), indicating that the ID-derived torque magnitude scaled more strongly with gravity level than the EMG-based estimates (Fig. 7A, left). For the peak-to-peak dynamic component, a significant main effect of gravity level ($F(1,2211) = 114.72, p = 3.9 \times 10^{-26}$) together with a strong method × gravity interaction ($F(1,2211) = 315.94, p = 3.6 \times 10^{-66}$; Fig. 7A, right) were observed, whereas the main effect of method alone was not significant ($F(1,2211) = 0.90, p = 0.34$; Supplementary Table S4) indicating different gravity-dependent scaling between EMG- and ID-derived torques. Consistent with these model results, participant-wise gravity-sensitivity slopes showed markedly different scaling patterns between torque components. Both components had significant effects of DOF and movement distance (Supplementary Table S3, S4) indicating joint-specific modulation of gravity-related torques (Supplementary Figure S3). Moreover, the gravity component exhibited steep subject-specific positive slopes in the ID-derived torques (median ≈ 32–33), reflecting strong proportional scaling with gravity level, whereas EMG-derived estimates showed substantially smaller positive slopes (median ≈ 14–15; Fig. 7B left). Conversely, the dynamic component displayed minimal gravity dependence in the ID estimates (slopes centered near zero), while EMG-derived torques exhibited moderate positive slopes (≈ 0.05–0.08), indicating increased dynamic-related muscle activity with increasing gravitational load (Fig. 7B right). Together, these results demonstrate that gravity-related and dynamic torque components exhibit distinct scaling

with gravitational conditions and that EMG-derived torques capture gravity-dependent modulations of muscle activation.

Supplementary Table S3: Gravity-related torque component linear mixed-effects model results

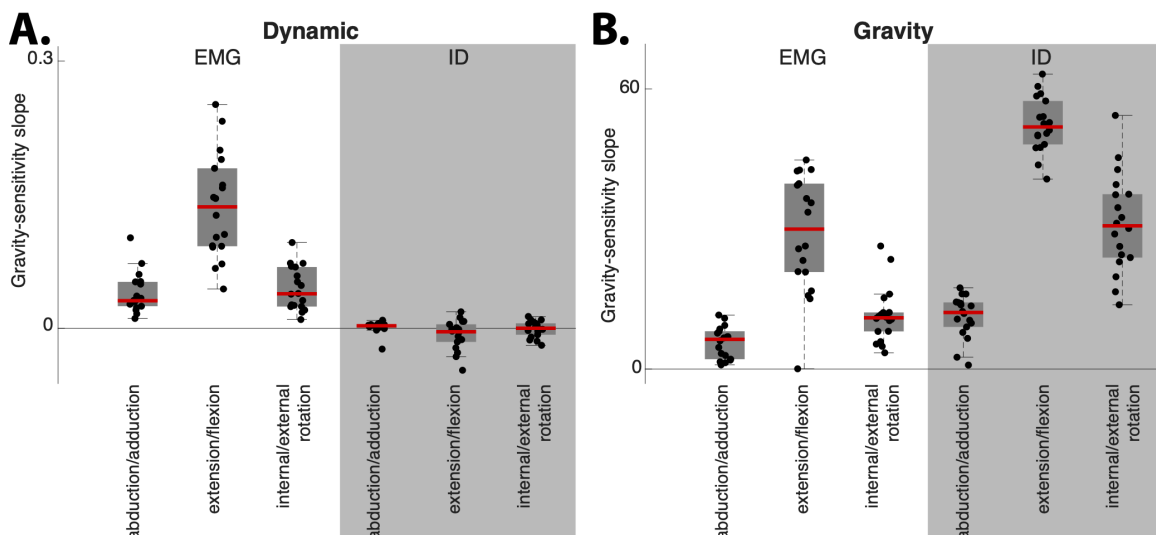
| Term | F | DF1 | DF2 | <i>p</i> |
|------------------|--------|-----|------|--------------|
| Intercept | 0.50 | 1 | 1491 | 0.477 |
| Method | 5.36 | 1 | 1491 | 0.021 |
| Gravity level | 0.11 | 1 | 1491 | 0.739 |
| DOF | 4.35 | 2 | 1491 | 0.013 |
| Distance | 87.55 | 1 | 1491 | 3e-20 |
| Method × Gravity | 147.89 | 1 | 1491 | 2e-32 |
| Gravity × DOF | 201.73 | 2 | 1491 | 3e-78 |

DOF – degree of freedom, 3 levels for shoulder extension/flexion, internal/external rotation, and abduction/adduction; Method refers to torque derivation, using inverse dynamics or from electromyography (EMG). Significant *p* values are in bold.

Supplementary Table S4: Dynamics-related torque component linear mixed-effects model results

| Term | F | DF1 | DF2 | <i>p</i> |
|------------------|--------|-----|------|---------------|
| Intercept | 15.23 | 1 | 2211 | 1e-04 |
| Method | 0.90 | 1 | 2211 | 0.343 |
| Gravity level | 114.72 | 1 | 2211 | 4e-26 |
| DOF | 471.17 | 2 | 2211 | 4e-171 |
| Distance | 116.92 | 1 | 2211 | 1e-26 |
| Method × Gravity | 315.94 | 1 | 2211 | 4e-66 |
| Gravity × DOF | 48.59 | 2 | 2211 | 2e-21 |

DOF – degree of freedom, 3 levels for shoulder extension/flexion, internal/external rotation, and abduction/adduction; Method refers to torque derivation, using inverse dynamics or from electromyography (EMG). Significant *p* values are in bold.



Supplementary Figure S3. Statistical analysis of torque metrics. A. Grouped distribution plot of subject-specific slopes per degree of freedom for dynamic component of joint torque. Symbols show individual participant slopes per method of metric derivation (EMG or ID), red lines show medians, grey boxes show interquartile ranges, dashed lines show total ranges. B. Same for the gravity component of joint torque.

EMG prediction coefficient statistics

To evaluate how biomechanical predictors contributed to muscle activation, regression coefficients associated with gravity torque, velocity, extension torque derivative, and flexion torque derivative were analyzed using linear mixed-effects models. The models included gravity condition (0g, 1g, 2g), movement direction (upward vs downward), and muscle (anterior and posterior heads of the deltoid, trapezius, and pectoralis) as fixed effects, with subject included as a random intercept. Coefficients differed across predictors, reflecting their relative contributions to the muscle activation profile (Fig. 9).

The gravity-related torque component accounted for sustained, gravity-dependent increases in muscle activation across all recorded muscles ($F(2,207) = 19.66$, $p = 1.52 \times 10^{-8}$), with coefficients increasing systematically from 0g to 2g (Fig. 9A; Supplementary Table S5). A significant main effect of movement direction was also observed ($F(1,207) = 9.92$, $p = 0.0019$), indicating differences between upward and downward movements. In addition, the gravity coefficient differed across muscles ($F(3,207) = 4.13$, $p = 0.0072$). No significant interaction effects were detected between gravity condition, movement direction, and muscle (all $p > 0.23$), suggesting that gravity-dependent modulation of this coefficient was consistent across muscles and movement directions.

Supplementary Table S5: Gravity coefficient linear mixed-effects model results

| Term | F | DF1 | DF2 | p |
|------------------------------------|-------|-----|-----|--------------|
| (Intercept) | 0.66 | 1 | 66 | 0.421 |
| Gravity Condition | 19.66 | 2 | 207 | 0.000 |
| Direction | 9.92 | 1 | 207 | 0.002 |
| Muscle | 4.13 | 3 | 207 | 0.007 |
| Gravity Condition:Direction | 0.62 | 2 | 207 | 0.538 |
| Gravity Condition:Muscle | 1.33 | 6 | 207 | 0.244 |
| Direction:Muscle | 1.44 | 3 | 207 | 0.232 |
| Gravity Condition:Direction:Muscle | 1.03 | 6 | 207 | 0.405 |

Two levels for Direction (upward and downward); Condition refers to gravity conditions (0g, 1g, 2g). Significant p values are in bold.

Joint angular velocity also contributed substantially to EMG prediction (Fig. 9B). Velocity coefficients varied less across gravity conditions ($F(2,216) = 2.82$, $p = 0.062$; Supplementary Table S6). They were larger during downward movements, with a significant main effect of movement direction ($F(1,216) = 14.46$, $p = 1.86 \times 10^{-4}$), indicating that velocity contributions to EMG differed between upward and downward movements. Velocity coefficients also differed across muscles ($F(3,216) = 3.70$, $p =$

0.0125), with the anterior deltoid and pectoralis exhibiting the largest values. No interaction terms were significant (all $p > 0.35$).

Supplementary Table S6: Velocity coefficient linear mixed-effects model results

| Term | F | DF1 | DF2 | p |
|------------------------------------|--------|-----|-----|--------------|
| (Intercept) | 137.58 | 1 | 216 | 7e-25 |
| Gravity Condition | 2.82 | 2 | 216 | 6e-02 |
| Direction | 14.46 | 1 | 216 | 2e-04 |
| Muscle | 3.70 | 3 | 216 | 1e-02 |
| Gravity Condition:Direction | 0.28 | 2 | 216 | 8e-01 |
| Gravity Condition:Muscle | 1.11 | 6 | 216 | 4e-01 |
| Direction:Muscle | 0.44 | 3 | 216 | 7e-01 |
| Gravity Condition:Direction:Muscle | 0.27 | 6 | 216 | 9e-01 |

Two levels for Direction (upward and downward); Condition refers to gravity conditions (0g, 1g, 2g). Significant p values are in bold.

Coefficients associated with direction-specific dynamic torque derivatives captured transient activation patterns related to propulsion and braking but explained less variance overall than the gravity-related torque or velocity terms (Fig. 9C,D). The flexion jerk coefficient showed a modest but significant dependence on gravity condition ($F(2,207) = 4.04$, $p = 0.0189$; Supplementary Table S7), whereas the extension jerk coefficient showed no significant dependence on gravity condition ($F(2,207) = 1.20$, $p = 0.302$; Supplementary Table S8). In contrast, a significant main effect of movement direction was observed for both the flexion jerk coefficient ($F(1,207) = 5.82$, $p = 0.0167$) and the extension jerk coefficient ($F(1,207) = 32.15$, $p = 4.75 \times 10^{-8}$), indicating that these dynamic components contributed differently during upward versus downward movements. The sign reversal of these coefficients was consistent with the task requirement to counteract deceleration interaction moments when terminating the movement (Fig. 9C,D). A significant effect of muscle was observed for the extension jerk coefficient ($F(3,207) = 3.79$, $p = 0.011$), but not for the flexion jerk coefficient ($F(3,207) = 0.99$, $p = 0.40$). None of the interaction effects were significant (all $p > 0.10$ for the extension jerk coefficient; all $p > 0.65$ for the flexion jerk coefficient).

Supplementary Table S7: Flexion torque derivative coefficient linear mixed-effects model results

| Term | F | DF1 | DF2 | p |
|------------------------------------|------|-----|-----|--------------|
| (Intercept) | 6.10 | 1 | 95 | 0.015 |
| Gravity Condition | 4.04 | 2 | 207 | 0.019 |
| Direction | 5.82 | 1 | 207 | 0.017 |
| Muscle | 0.99 | 3 | 207 | 0.400 |
| Gravity Condition:Direction | 0.08 | 2 | 207 | 0.923 |
| Gravity Condition:Muscle | 0.70 | 6 | 207 | 0.652 |
| Direction:Muscle | 0.21 | 3 | 207 | 0.887 |
| Gravity Condition:Direction:Muscle | 0.33 | 6 | 207 | 0.922 |

Two levels for Direction (upward and downward); Condition refers to gravity conditions (0g, 1g, 2g). Significant p values are in bold.

Supplementary Table S8: Extension torque derivative coefficient linear mixed-effects model results

| Term | F | DF1 | DF2 | p |
|------------------------------------|-------|-----|-----|--------------|
| (Intercept) | 8.46 | 1 | 113 | 0.004 |
| Gravity Condition | 1.20 | 2 | 207 | 0.302 |
| Direction | 32.15 | 1 | 207 | 0.000 |
| Muscle | 3.79 | 3 | 207 | 0.011 |
| Gravity Condition:Direction | 2.25 | 2 | 207 | 0.108 |
| Gravity Condition:Muscle | 0.74 | 6 | 207 | 0.618 |
| Direction:Muscle | 0.42 | 3 | 207 | 0.741 |
| Gravity Condition:Direction:Muscle | 0.56 | 6 | 207 | 0.761 |

Two levels for Direction (upward and downward); Condition refers to gravity conditions (0g, 1g, 2g). Significant p values are in bold.